CHEMISTRY
A EUROPEAN JOURNAL

DOI: 10.1002/chem.200500338

VIP

When are Two Waters Worse Than One? Doubling the Hydration Number of a Gd–DTPA Derivative Decreases Relaxivity

Peter Caravan,*[a] John C. Amedio Jr.,[a] Stephen U. Dunham,[a] Matthew T. Greenfield,[a] Normand J. Cloutier,[a] Sarah A. McDermid,[a] Marga Spiller,[b] Stephan G. Zech,[a] Richard J. Looby,[a] Arnold M. Raitsimring,[c] Thomas J. McMurry,[a] and Randall B. Lauffer[a]

Dedicated to Professor André Merbach on the occasion of his 65th birthday

Abstract: The synthesis of a novel ligand, based on *N*-methyl-diethylenetriaminetetraacetate and containing a diphenylcyclohexyl serum albumin binding group (**L1**) is described and the coordination chemistry and biophysical properties of its Gd^{III} complex **Gd–L1** are reported. The Gd^{III} complex of the diethylenetriaminepentaacetate analogue of the ligand described here (**L2**) is the MRI contrast agent MS-325. The effect of converting an acetate to a methyl group on metal–ligand stability, hydration number, water-exchange rate, relaxivity, and binding to the protein human serum albumin (HSA) is explored. The complex **Gd–L1** has two coordinated water molecules in solution, that is, $[Gd(\mathbf{L1})(H_2O)_2]^{2-}$ as shown by D-band proton ENDOR spectroscopy and implied by ^1H and ^{17}O NMR relaxation rate measurements. The $Gd{-}H_{water}$ distance of the coordinated waters was found to be identical to that found for **Gd–L2**, 3.08 Å. Loss of the acetate group destabilizes the Gd^{III} complex by 1.7 log units ($\log K_{ML} = 20.34$) relative to the complex with **L2**. The affinity of **Gd–L1** for HSA is essentially the same as that of **Gd–L2**. The water-exchange rate of the two coordinated waters on **Gd–L1** ($k_{ex} = 4.4 \times 10^5\ s^{-1}$) is slowed by an order of magnitude relative to **Gd–L2**. As a result of this slow water-exchange rate, the observed proton relaxivity of **Gd–L1** is much lower in a solution of HSA under physiological conditions ($r_1^{obs} = 22.0\ mM^{-1}s^{-1}$ for 0.1 mM **Gd–L1** in 0.67 mM HSA, HEPES buffer, pH 7.4, 35 °C at 20 MHz) than that of **Gd–L2** ($r_1^{obs} = 41.5\ mM^{-1}s^{-1}$) measured under the same conditions. Despite having two exchangeable water molecules, slow water exchange limits the potential efficacy of **Gd–L1** as an MRI contrast agent.

Keywords: gadolinium · imaging agents · magnetic resonance imaging · relaxivity · serum albumin

Introduction

Magnetic resonance imaging (MRI) is a firmly established clinical technique that provides noninvasive high-resolution images of body tissues. Clinical MRI measures the NMR signals of protons, largely those of water. Differences in signal intensity create contrast in the image and may allow discrimination between tissue types and disease states. Tissue contrast is achieved in many ways—by means of differences in water content among tissues, by weighting the imaging sequence to display differences in proton relaxation rates ($1/T_1$ and $1/T_2$), differences in chemical shift, differences in water diffusion, the effect of flowing blood, or by using magnetization-transfer techniques.[1] In T_1-weighted imaging, a more intense signal is observed in regions in which the longitudinal relaxation rate is fast (for which T_1 is

[a] Dr. P. Caravan, Dr. J. C. Amedio Jr., Dr. S. U. Dunham, M. T. Greenfield, Dr. N. J. Cloutier, S. A. McDermid, Dr. S. G. Zech, R. J. Looby, Dr. T. J. McMurry, Dr. R. B. Lauffer
EPIX Pharmaceuticals, Inc., 67 Rogers Street
Cambridge, MA 02142–1118 (USA)
Fax: (+1) 617-250-6127
E-mail: pcaravan@epixpharma.com

[b] M. Spiller
Department of Radiology, New York Medical College
Valhalla, NY 10595 (USA)

[c] Dr. A. M. Raitsimring
Department of Chemistry, University of Arizona
Tucson, AZ 85721 (USA)

short). The longitudinal relaxation rate of water protons can be further enhanced by the addition of paramagnetic metal complexes. These complexes, known as MRI contrast agents,[2] provide enhanced image contrast in regions in which the complex localizes.

The first generation of clinically approved contrast agents distribute to plasma and to the extracellular space.[3] These are low-molecular-weight ternary complexes of gadolinium(III), in which the Gd^{III} ion is complexed by an octadentate ligand and a single coordinated water molecule. The octadentate ligand is required for safety—to insure that the somewhat toxic Gd^{III} ion remains sequestered in vivo and that the complex can be excreted intact. The coordinated water is required for contrast. The Gd^{III} ion relaxes the coordinated water, which is in fast exchange with bulk water. This results in a shortened T_1 value for the bulk (and MRI observable) water.

MS-325 (also referred to here as **Gd–L2**) is a new contrast agent[4] that has recently completed clinical trials for blood vessel imaging.[5] MS-325 was designed to reversibly target the protein human serum albumin (HSA) in the blood plasma.[6] Binding to HSA serves three purposes: 1) it restricts the distribution of the contrast agent to the intravascular space, 2) reversible binding insures that there is always an unbound fraction available for renal excretion, and 3) it enhances the relaxivity of the compound. Relaxivity (r_1) refers to the ability of the complex to enhance the relaxation rate of the solvent; see Equation (1) in which $\Delta(1/T_1)$ is the change in relaxation rate of the solvent after addition of contrast agent of metal concentration [M] in units of mM.

$$r_1 = \frac{\Delta(1/T_1)}{[\mathrm{M}]} \tag{1}$$

At equal concentration, a compound with enhanced relaxivity will appear brighter in an image compared to a compound of lower relaxivity; alternately a compound with higher relaxivity can provide the same contrast as a low relaxivity compound but at a lower dose.

Relaxivity can be factored into a term that accounts for the relaxation effect due the coordinated inner-sphere water (r_1^{IS}) and an outer-sphere term (r_1^{OS}), which encompasses contributions of relaxation to the second and outer-sphere waters [Eq. (2)]. The inner-sphere term is given by Equation (3), which is derived from the description of two-site exchange.[7]

$$r_1 = r_1^{IS} + r_1^{OS} \tag{2}$$

$$r_1^{IS} = \frac{q/[H_2O]}{T_{1m} + \tau_m} \tag{3}$$

Here q is the number of coordinated water molecules, the water concentration is in mM, T_{1m} is the relaxation time of the coordinated water(s), and τ_m is the lifetime of the coor-

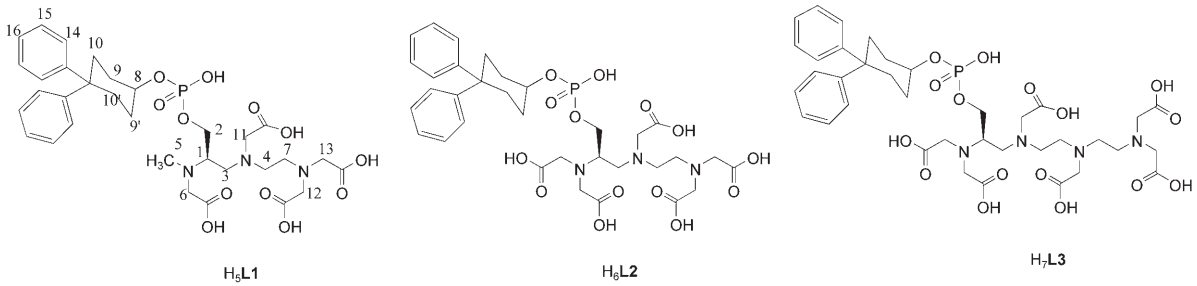

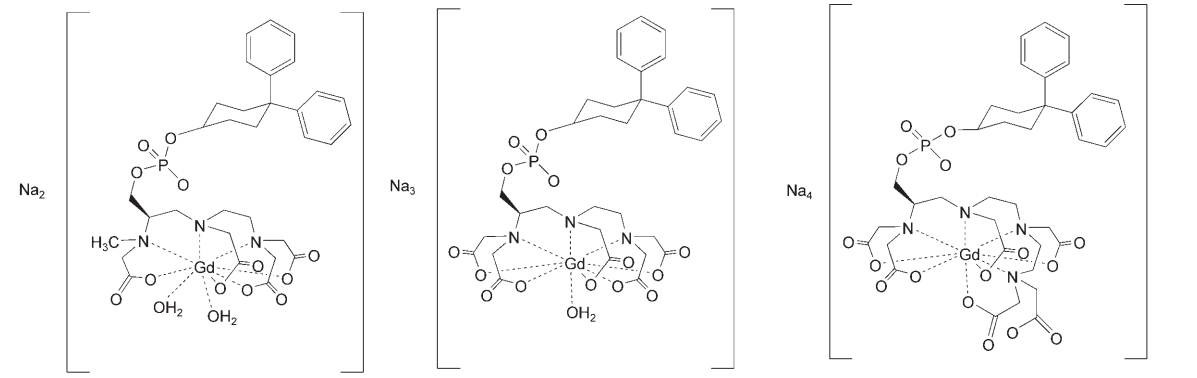

dinated water (inverse of the water-exchange rate, $k_{ex}=1/\tau_m$).

It is apparent from Equation (3) that the relaxivity can be increased by increasing the number of coordinated water molecules or by decreasing the denominator. It was recognized early on that the relaxivity at clinical field strengths of compounds like $[Gd(DTPA)(H_2O)]^{2-}$ is limited by T_{1m}.[8] The reason for this is that the rotational diffusion rate of the complex is very fast compared to the Larmor frequency of the hydrogen atom. When MS-325 forms an adduct with HSA, the rotational diffusion rate is slowed and the relaxation efficiency of the inner-sphere water is enhanced (T_{1m} is decreased). This leads to a relaxivity of MS-325 in blood plasma that is several times the relaxivity obtained in pure water.[4]

In early mechanistic studies of Gd^{III}-based contrast agents it was assumed that the water-exchange rate was very fast and close to the diffusion limit. However in a series of seminal papers in the 1990s, the Merbach research group in Lausanne showed that the water-exchange rate depended on the co-ligand and that this rate could vary over several orders of magnitude.[9–14] For the Gd^{III} compounds used clinically, water-exchange rates were 2–3 orders of magnitude slower than that on the aqua ion. Yet since relaxation of the coordinated water was not very efficient due to fast rotation, $T_{1m} \gg \tau_m$, and the relaxivities of these compounds are essentially the same.[2]

For protein-targeted or for polymeric gadolinium complexes it is expected that the water-exchange rate may be the limiting factor for optimizing relaxivity. During the development of the synthetic process for MS-325 it was observed that if the borane reduction of a protected amide intermediate was carried out under reflux conditions (vide infra), the protecting group is lost and an *N*-methyl impurity forms. Carrying this impurity through the alkylation and complexation conditions used for MS-325 yields a compound denoted **Gd–L1**. Compound **Gd–L1** is a useful model for mechanistic studies. The similarity to MS-325 (referred to hereafter as **Gd–L2**) suggests that it will bind to albumin at the same site. The albumin-bound relaxivity of **Gd–L1** should differ from **Gd–L2**, because there are two coordinated water molecules and the water-exchange rate is expected to be different as the co-ligand has changed.

This paper reports on the synthesis of **Gd–L1**, its affinity for serum albumin, its water-exchange rate, the field- and temperature-dependent relaxivities in buffer only and in buffered solutions of HSA. In addition, the Gd–H distance is estimated from a D-band ^1H ENDOR study and compared to that of **Gd–L2**. Finally the effect of modifying the DTPA core ligand on the formation constant of the Gd^{III}, Zn^{II}, and Ca^{II} complexes is assessed.

Results and Discussion

The synthesis of the ligand H_5**L1** and its gadolinium(III) complex **Gd–L1** is outlined in Scheme 1. Compound **1**,[16] a key intermediate in the preparation of MS-325,[15] was treated with a borane–tetrahydrofuran complex under reflux conditions to achieve amide and carbamate reduction, yielding *N*-methyl triamine **2**. The triamine compound **2** was tetraalkylated by heating with *tert*-butyl bromoacetate in dimethylformamide with diisopropylethylamine as an acid scavenger and potassium iodide as a reaction catalyst. Compounds **3** and **4** were coupled together through a phosphate diester link to give ligand H_5**L1**. This was accomplished by reacting compound **4** and phosphorus trichloride together in tetrahydrofuran to generate 4,4-diphenylcyclohexyl dichlorophosphite in situ. The dichlorophosphite was activated by reaction with imidazole and the resultant diimidazolide was reacted with compound **3** to afford a tetra-*tert*-butyl ester of [(diphenylcyclohexyl)phosphinooxymethyl]-*N*-methyldiethylenetriamine tetraacetic acid as an intermediate. In situ oxidation of the phosphorus atom with sodium periodate followed by deprotection of the *tert*-butyl ester groups with concentrated hydrochloric acid afforded H_5**L1**. This sequence converted alcohols **3** and **4** to H_5**L1** in one-

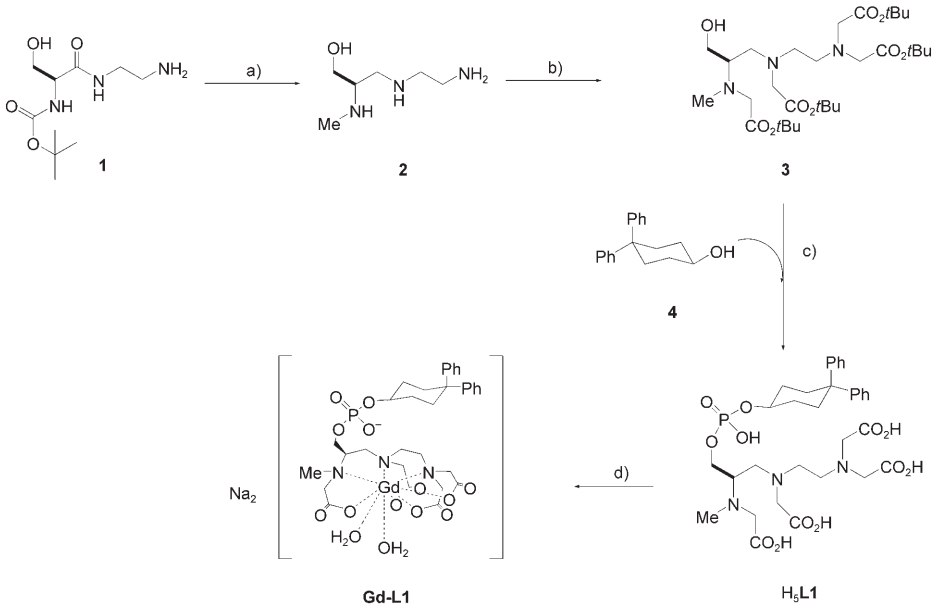

Scheme 1. a) BH_3–THF, reflux. b) diisopropylethylamine, KI, DMF, $BrCH_2CO_2C(CH_3)_3$. c) i) PCl_3, THF; ii) **4**, THF; iii) imidazole; iv) **3**; v) $NaIO_4$, aq. HCl; vi) conc. HCl. d) $GdCl_3$, aq. NaOH.

pot, utilizing five synthetic steps. Reaction with a stoichiometric amount of Gd^{III} and adjusting the pH to neutral with sodium hydroxide yields **Gd–L1**.

The regiochemistry of H_5**L1** was investigated by means of heteronuclear ^1H-^{13}C correlation spectroscopy. The methyl group and the two CH groups can be easily identified in a multiplicity-edited HSQC spectrum, since they show opposite intensity from CH_2 groups. The location of the *N*-methyl group is confirmed by the observation of a long-range J(C–H) coupling to the carbon atom at the 1-position (see graphic above for atom labeling) in the HMBC experiment. Assignment of the proton chemical shifts was obtained from DQF-COSY, TOCSY, and ROESY experiments that complemented the carbon shifts derived from HSQC and HMBC experiments.

The ligand H_5**L1** was isolated from acid in its neutral form. Titration of H_5**L1** shows that it has five ionizable protons (Figure 1) with protonation constants listed in Table 1.

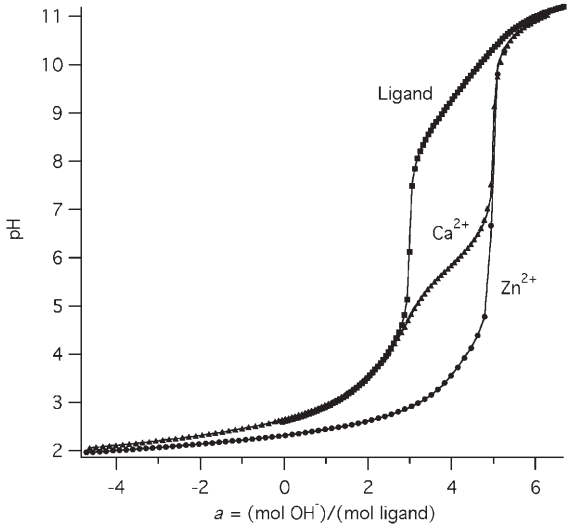

Figure 1. Observed pH versus a (mol OH^-/mol ligand) at 1 M:1 **L1** ratios, 25 °C, $\mu = 0.1$ M $NaClO_4$, [M] = [L] ~ 1.5 mM. Symbols are measured pH and solid lines are fits using the equilibria in Tables 1 and 2.

Table 1. Protonation constants for **L1** and comparison with **L2**[26] determined at 25 °C in 0.1 M $NaClO_4$. Numbers in parentheses refer to 1 standard deviation based on mean of 4 titrations consisting of >100 data points.

Log K	**L1**	**L2**
[HL1]/[H][L1]	9.84 (0.01)	9.56
[H_2L1]/[H][HL1]	8.73 (0.01)	8.31
[H_3L1]/[H][H_2L1]	3.93 (0.03)	4.41
[H_4L1]/[H][H_3L1]	2.57 (0.04)	2.92
[H_5L1]/[H][H_4L1]	1.92 (0.09)	2.43

The basicity of the ligand is in line with what might be expected for a diethylenetriamine substituted with acetate groups. Two of the nitrogen atoms are considerably basic ($pK_a > 8.5$), while the third nitrogen atom and the carboxylate groups are more acidic. The protonation constants for H_6**L2** determined under the same conditions[26] are also listed in Table 1 for comparison. The addition of the *N*-methyl substituent makes this nitrogen atom of **L1** more basic than that of **L2**.

Once the protonation constants were determined it was possible to determine some stability constants with different metals. The Ca^{II} and Zn^{II} stability constants were determined by direct titration of a 1:1 mixture of metal and ligand. Figure 1 shows that the Ca^{II} complexes (**Ca–L1** and **HCa–L1**) are rather weak and are only significantly formed at pH > 5. The Zn^{II} complex on the other hand is formed at a much lower pH. The **Gd–L1** stability constant could not be determined by direct titration because the complex precipitated (presumably as a protonated form) at the low pH (pH < 2.5) needed to have a mixture of free ligand and free metal ion. The stability constant was determined by competition for Gd^{III} with **L1** and the EDTA ligand. The diphenylcyclohexyl moiety on **L1** enables it to be retained on a reverse phase HPLC column and allows the gadolinium complex to be separated from the free ligand. Quantitative HPLC-MS of **Gd–L1** and H_n**L1** along with knowledge of the ligand protonation constants, the pH, and the Gd–EDTA stability constant enables calculation of the **Gd–L1** formation constant.

The stability constants for **M–L1** are listed in Table 2 along with the stability constants for **M–L2** reported previously under the same conditions (ionic strength, medium, temperature).[26] The stability constant for **Gd–L1** is 1.7 log units lower than that of **Gd–L2**. A lower stability may be expected from removing one of the coordinating acetate groups from **L2** and replacing it with a noncoordinating methyl group. Even with the drop in stability, **Gd–L1** still forms a significantly more stable complex than the commercial contrast agent Gd–DTPA–BMA ($\log K_{ML} = 16.85$).[27] The oxophilic calcium(II) ion also has a slightly lower stability constant with **L1** relative to that observed with **L2**. On the other hand, **Zn–L1** is more stable than **Zn–L2**. This is probably because of the lower coordination number of Zn^{II} relative to those of Ca^{II} and Gd^{III}. The Zn^{II} ion does not require the fifth acetate oxygen donor atom. The increased basicity of the nitrogen donor as a result of the methyl substitution could explain the increased **Zn–L1** stability constant relative to **Zn–L2**.

Table 2. Stability constants and metal complex protonation constants for Gd^{III}, Ca^{II}, and Zn^{II} binding to **L1** and comparative values for the **M–L2** complexes.[26] Equilibria determined at 25 °C, 0.1 M $NaClO_4$. Values in parentheses refer to 1 standard deviation.

Log K	**L1**	**L2**
[GdL]/[Gd][L]	20.34 (0.04)	22.06
[CaL]/[Ca][L]	10.16 (0.02)	10.45
[HCaL]/[H][CaL]	5.70 (0.005)	5.66
[ZnL]/[Zn][L]	18.42 (0.03)	17.82
[HZnL]/[H][ZnL]	4.01 (0.005)	5.60
[H_2ZnL]/[H][HZnL]	1.83 (0.02)	2.54

The **Gd–L1** complex used for further characterization was prepared in situ by mixing stoichiometric amounts of H_5**L1** and $GdCl_3$ and adjusting the pH to 7 with NaOH. The absence of excess gadolinium was confirmed by titration with xylenol orange. The HPLC-MS trace of the solution showed a single peak with a mass corresponding to the parent ion of **Gd–L1**.

It is expected that **Gd–L1** would be nine-coordinate with two bound water molecules ($q=2$), that is $[Gd(\mathbf{L1})(H_2O)_2]^{2-}$. This is analogous to **Gd–L2**, which was shown to be nine-coordinate in solution[6] as are other gadolinium(III)–DTPA derivatives.[28–32] It was recently shown that gadolinium ENDOR spectroscopy is a useful method to determine the distance between the Gd^{III} ion and the coordinated water oxygen atom[24] or protons.[23,25] Figure 2 shows

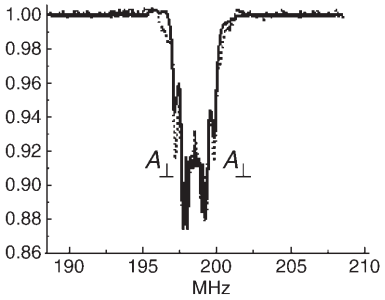

Figure 2. Normalized (to unity) D-band proton ^{1}H ENDOR spectrum corresponding to the $-1/2\leftrightarrow+1/2$ electronic transition. The spectrum for **Gd–L1** is shown by a dotted line and the **Gd–L2** spectrum is superimposed as a solid line.

the frozen solution D-band proton ENDOR spectrum corresponding to the $-1/2\leftrightarrow+1/2$ electronic transition. The spectrum for **Gd–L1** is shown by a dotted line and the **Gd–L2** spectrum is superimposed as a solid line. The two spectra are superimposable except for the shoulders at about 197 and 200 MHz, which are labeled $A_\perp$. These shoulders correspond to the perpendicular part of the hyperfine coupling constant to coordinated water molecules. The central features of the spectrum arise from protons more distant from the Gd atom, that is; protons on the co-ligand and protons from the solvent matrix. The shoulders occur at identical frequencies indicating that **Gd–L1** and **Gd–L2** have the same hyperfine coupling to coordinated water molecules and the same $Gd{-}H_{water}$ distance.[23,25] This results in a $Gd{-}H_{water}$ distance of 3.08 Å. As discussed previously, the width of this shoulder indicates that the $Gd{-}H_{water}$ distance is distributed within ±0.1 Å and centered at 3.08 Å. The significantly greater intensity of the $A_\perp$ shoulder for **Gd–L1** relative to **Gd–L2** is qualitative evidence to show that **Gd–L1** has two bound water molecules in solution. The ENDOR spectrum of **Gd–L1** in the presence of HSA (not shown) has the same $A_\perp$ shoulder that occurs at the same frequency and at the same amplitude as for **Gd–L1** in water. This implies that the hydration number does not change when **Gd–L1** is bound to HSA.

The affinity of **Gd–L1** for HSA is very similar to that reported for **Gd–L2** (MS-325). Under the conditions of 0.1 mM **Gd–L1** and 4.5% (w/v) HSA in pH 7.4 phosphate-buffered saline, **Gd–L1** was 89.4 ± 0.4% bound to albumin. Under identical conditions, **Gd–L2** was 88% bound to albumin.[6] This is not surprising given the common binding group. The difference in charge on the complex appears to play no role. There was no measurable effect of temperature on albumin binding. The binding assay was repeated at 5°C and the **Gd–L1** was 89.4% bound at this temperature as well.

Like **Gd–L2**, **Gd–L1** also binds to site II on HSA; this is binding site on subdomain IIIA at which the anti-inflammatory drugs ibuprofen and naproxen bind. By using a fluorescent probe displacement assay described previously, it was found that **Gd–L1** displaces the probe dansylsarcosine from HSA with an inhibition constant, $K_i=100\pm10\,\mu M$ (K_i for **Gd–L2** $=85\,\mu M$).[6] Using this K_i value, it was calculated that under the conditions of 0.1 mM **Gd–L1** and 4.5% HSA (0.67 mM) there should be 85% of **Gd–L1** bound to site II. The measured value of 89.4% suggests that **Gd–L1** is primarily bound to site II. A site I probe was also tested. Dansyl-L-asparagine is known to bind to site I. **Gd–L1** showed only very weak displacement of the site I probe: $K_i=3000\pm1000\,\mu M$ (K_i for **Gd–L2** $=1500\,\mu M$).[6]

The relaxivities of **Gd–L1**, **Gd–L2**, and **Gd–L3** in HEPES buffer or in 4.5% HSA solution in HEPES buffer at 35°C (pH 7.4, 20 MHz) are shown graphically in Figure 3.

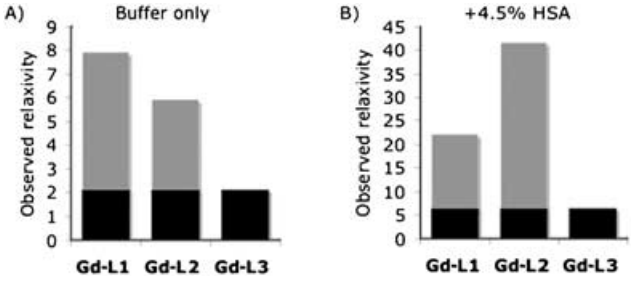

Figure 3. Observed relaxivities of **Gd–L1**, **Gd–L2**, and **Gd–L3** in A) HEPES buffer and B) HEPES buffer + 4.5% (w/v) HSA at 35°C, 20 MHz, pH 7.4. The estimated second- and outer-sphere relaxivity component is shown in black and the estimated inner-sphere component in gray.

The relaxivity of the $q=0$ **Gd–L3** complex serves as an estimate of the second and outer-sphere contributions to relaxivity. The bar graphs show this second/outer-sphere effect in black, and the gray part represents the estimate of relaxivity due to the inner-sphere water. In buffer alone, the relaxivity of **Gd–L1** is higher than that of **Gd–L2**, consistent with **Gd–L1** having two coordinated water molecules, although the inner-sphere effect is only 50% greater for **Gd–L1**. When HSA is added, the relaxivities increase for all compounds. Now, however, the relaxivity of the $q=1$ **Gd–L2** is clearly much larger than that of **Gd–L1**. The relaxivities reported are all "observed relaxivities", this is the relaxivity that was calculated based on the measured relaxation rates

and arises from both the albumin-bound and free fractions of the complexes. As shown above, the albumin affinity is the same, so this difference in relaxivity does not arise in a difference in the fraction bound to albumin.

Variable-temperature ^{17}O relaxation-rate studies proved critical in understanding the proton relaxivity differences. Figure 4 shows the reduced relaxation-rate data, $1/T_{1r}$ and

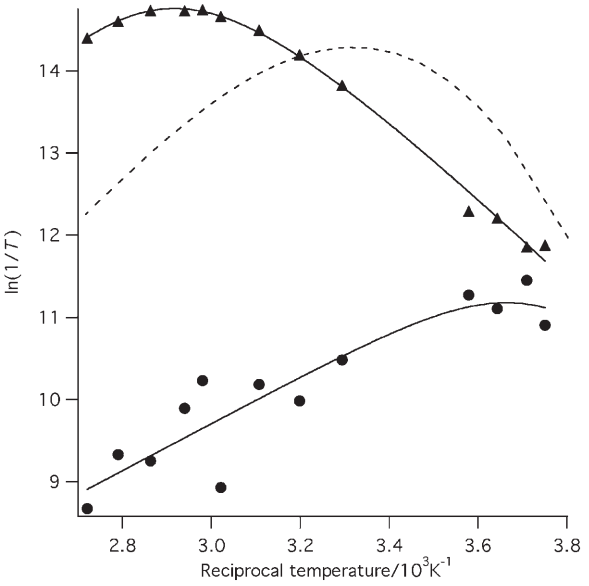

Figure 4. Reduced ^{17}O relaxation rates ($1/T_{1r}$, circles and $1/T_{2r}$, triangles) of $H_2{}^{17}O$ in the presence of **Gd–L1** vs reciprocal temperature. Solid lines represent the simultaneous fit to the data. The dashed line represents the $1/T_{2r}$ data for **Gd–L2** that was described previously.

$1/T_{2r}$, for **Gd–L1** as a function of reciprocal temperature. The scatter in the $1/T_{1r}$ data is greater than that in the $1/T_{2r}$ data because fast rotation (vide infra) leads to only a small paramagnetic enhancement, whereas the paramagnetic scalar contribution to transverse relaxation is quite large. As a result, the ^{17}O $1/T_1$ values determined in the presence of **Gd–L1** are close in magnitude to the those of the solvent alone, and the difference between the two results in a much larger relative error for $1/T_{1r}$ than for $1/T_{2r}$.

The data were analyzed as described previously[6] and the fitted parameters are listed in Table 3 along with the corresponding values for **Gd–L2**. The hyperfine coupling constant between the Gd and the $H_2{}^{17}O$ was fixed at -3.8×10^6 rad s^{-1}.[12] The rotational correlation time at 37 °C determined by ^{17}O NMR for **Gd–L1** was very similar to that obtained for **Gd–L2**; this result is expected given the close similarity between the molecules. The striking difference was in the water-exchange rate. The water-exchange rate for **Gd–L1** is markedly reduced relative to that of **Gd–L2**, going from 5.8×10^6 s^{-1} for **Gd–L2**[6] at 298 K to 0.44×10^6 s^{-1} for **Gd–L1**. In Figure 4 the dashed line represents the $1/T_{2r}$ data for **Gd–L2**; this line highlights the large difference in water exchange between the two complexes. At lower temperatures (right side of graph) $1/T_{2r}$ approaches k_{ex} and

Table 3. Parameters obtained from the simultaneous fit of T_1 and T_2 relaxation rate data for $H_2{}^{17}O$ in the presence of **Gd–L1** and **Gd–L2** (MS-325).[6] Numbers in parentheses refer to one standard deviation.

	Gd–L1	**Gd–L2** (MS-325)[6]
τ_m^{37} [ns]	1160 (600)	69
k_{ex}^{298} [$\times10^6$ s^{-1}]	0.44 (0.21)	5.8
$\Delta H^{\neq}$ [kJ mol^{-1}]	40.0 (9.5)	53.7
$\Delta S^{\neq}$ [J K^{-1} mol^{-1}]	−3 (30)	+65
$1/T_{1e}^{37}$ [$\times10^7$ s^{-1}]	2.3 (2.6)	5.0
$\Delta E_{T_{1e}}$ [kJ mol^{-1}]	−15 (28)	−7.7
τ_R^{37} [ps]	118 (10)	115
ΔE_R [kJ mol^{-1}]	24.2 (4.4)	31.5

Figure 4 clearly shows a large difference in water-exchange rate.

The slow water-exchange rate has a profound effect on relaxivity. For a compound tumbling rapidly at 35 °C ($\tau_R=$ 115 ps), T_{1m} is on the order of 5.2 μs at 20 MHz. The water residency time τ_m is normally on the nanosecond timescale and the denominator in Equation (3) is dominated by T_{1m}. This is certainly true for **Gd–L2** in which the water exchange has no effect on limiting relaxivity. For **Gd–L1** however, $\tau_m=1.3$ μs at 35 °C and now the long water residency time contributes 20% to the denominator in Equation (3) resulting in a lower than expected relaxivity for **Gd–L1** even in HEPES buffer. The long water residency time for **Gd–L1** provides an upper limit on the expected inner-sphere relaxivity for this compound. If the relaxation time of the coordinated water, T_{1m}, was made very short, the inner-sphere relaxivity of **Gd–L1** would be at most 27.7 mM^{-1}s^{-1}. The slow water-exchange result means that although **Gd–L1** has two exchangeable water molecules, its relaxivity is lower in HSA than **Gd–L2** with one rapidly exchanging water molecule.

The slow water-exchange kinetics predict that the inner-sphere relaxation effect should be almost completely shut down if the solutions are cooled down. This is shown in Figure 5, in which the NMRD profiles of **Gd–L1**, **Gd–L2**, and **Gd–L3** are shown in buffer and in HSA solution at 35 °C and at 5 °C. At 5 °C the water residency times for **Gd–L1** and **Gd–L2** are 7.8 and 0.9 μs, respectively, giving upper limits on inner-sphere relaxivity of 4.6 and 20 mM^{-1}s^{-1}, respectively. Using the relaxivity of **Gd–L3** as an estimate of second/outer-sphere relaxivity, one sees that slow water exchange almost completely limits the relaxivity of **Gd–L1** at low temperature. The relaxivity of **Gd–L1** in HSA at 5 °C is very similar to that of **Gd–L3**, demonstrating that at this low temperature most of the relaxation enhancement arises from water protons in the second sphere. Even in buffer alone, the relaxivity of **Gd–L1** is lower than that of **Gd–L2**, because of slow exchange of the inner-sphere water.

It is not clear why replacing the N-terminal acetate group with a methyl group has such a dramatic effect on the water-exchange rate. One possible explanation is that the charge is reduced in going from **Gd–L2** to **Gd–L1** making the Gd^{III} ion more acidic and strengthening the Gd–O bond.

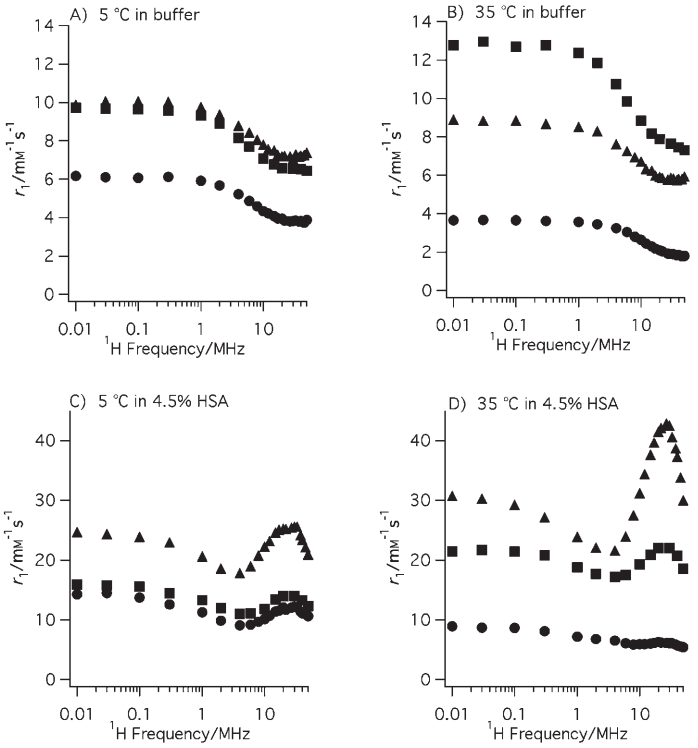

Figure 5. NMRD profiles showing observed relaxivities of **Gd–L1** (squares), **Gd–L2** (triangles), and **Gd–L3** (circles) at pH 7.4 in A) HEPES buffer, 5 °C, B) HEPES buffer, 35 °C, C) HEPES buffer + 4.5% (w/v) HSA, 5 °C, D) HEPES buffer + 4.5% (w/v) HSA, 35 °C.

This is not likely. The ENDOR measurement clearly showed that there was no change in the Gd−H_{water} distance. If the Gd−O_{water} bond was shorter for **Gd–L1** than **Gd–L2** one would expect the proton distance to change as well. It is worthwhile to consider a related system. Consider removal of an acetate group from $[Gd(DOTA)(H_2O)]^-$ to give $[Gd(DO3A)(H_2O)_2]$ (DOTA = 1,4,7,10-tetraazacyclododecane-1,4,7,10-tetraacetato, DO3A = 1,4,7,10-tetraazacyclododecane-1,4,7-triacetato). Again the charge is reduced and there are now two waters bound, but in this case the water-exchange rate *increases* for $[Gd(DO3A)(H_2O)_2]$.[12,33] It may simply be that an eight-coordinate transition state (assuming a dissociative mechanism) is less stable in the case of **Gd–L1** than for **Gd–L2**. Future work should address obtaining X-ray crystal structures of **Gd–L1** and **Gd–L2**.

Conclusion

Removal of one of the acetate oxygen donor atoms from the MRI contrast agent MS-325 (**Gd–L2**) and replacement with a methyl group to give **Gd–L1** results in a complex with two coordinated water molecules that still has relatively high thermodynamic stability. However because of the slow water-exchange rate of these two water molecules, the relaxivity of this compound in buffered serum albumin solution is much lower than may have been expected, and is considerably worse than MS-325 itself.

Experimental Section

Materials: Human serum albumin (HSA), product number A-1653 (Fraction V Powder 96–99% albumin, containing fatty acids), and the fluorescent probes dansyl-L-asparagine, and dansylsarcosine (piperidinium salt), were purchased from Sigma Chemical Co. (St. Louis, Mo.). Ultrafiltration units (UFC3LCC00, regenerated cellulose membrane of 5,000 Dalton nominal molecular weight cut-off) were obtained from Millipore Corporation (Bedford, MA). Other reagents were supplied by Aldrich Chemical Co., and were used without further purification. Solvents (HPLC grade) were purchased from various commercial suppliers as used as received. Column chromatography was conducted using silica gel from EM Merck. The compounds **Gd–L2** (MS-325)[15] and **Gd–L3**[6] were synthesized as described previously. NMR spectra of synthetic intermediates were obtained with a Varian Unity 300 or a Bruker Avance 400 spectrometers.

Preparation of compound 2: A round-bottomed flask, equipped with an addition funnel, temperature probe, and a nitrogen purge was charged with THF (100 mL) and compound **1**[16] (10.0 g, 40.4 mmol). The borane–THF complex (1 M solution, 202 mL, 5 equiv, 202 mmol) was added over a period of 30 min while maintaining an internal temperature of 25–30 °C. The reaction mixture was heated to 60–65 °C (reflux) and the mixture was allowed to stir for 7 days. The reaction mixture was cooled to room temperature. Then aqueous HCl (2 N, 24 mL) was added, followed by concentrated HCl (16 mL) while maintaining an internal temperature of 25–30 °C. The solvent (THF) was removed under vacuum (15 mm Hg, 40–45 °C water bath) to obtain a mobile oil. The oil was heated to 90–95 °C and allowed to stir for 18 h. The mixture was cooled to room temperature and the solids (boric acid) were collected by suction filtration. The filtrate was concentrated under vacuum (1 mm Hg, 40–45 °C water bath) to obtain a pasty solid, which was combined with ethanol (50 mL) to facilitate precipitation. The solids were collected by suction filtration and washed with ethanol (3 × 100 mL), recrystallized with 25% *n*-butanol in ethanol and dried to provide 5.5 g of compound **2**. ^{1}H NMR: (D_2O): δ = 2.7 (s, 3H), 3.2–3.4 (m, 6H), 3.5–3.6 (m, 1H), 3.7–3.9 ppm (m, 2H).

Preparation of compound 3: A round-bottomed flask, equipped with an addition funnel, temperature probe, and a nitrogen purge was charged with DMF (500 mL), compound **2** (15.0 g), potassium iodide (19.4 g, 2.0 equiv) and diisopropylethylamine (152.0 mL, 15.0 equiv). The mixture was cooled to 0–5 °C and *tert*-butyl bromoacetate (60.8 mL, 7 equiv) was added over a period of 30 min, while maintaining an internal temperature of 5–10 °C. The reaction mixture was allowed to warm to room temperature, and stirring continued for 24 h. The mixture was cooled to 0–5 °C and aqueous HCl (3 N, 250 mL) was added over a period of 15 min, while maintaining an internal temperature of 5–10 °C. Heptane (350 mL) was added and the mixture was stirred for 20 min. The layers were separated and the aqueous layer (pH 3) was treated with saturated sodium carbonate until pH 7 was achieved. Heptane (250 mL) was combined with the neutralized aqueous layer and stirred for 20 min. The layers were separated. The organic layer was dried over $MgSO_4$ and filtered, and the solvent was removed under vacuum (15 mm Hg, 40–45 °C water bath) to give a crude oil (22.0 g). The oil was subjected to silica gel chromatography (25% ethyl acetate/75% hexanes solvent system) to provide purified compound **3** (14.0 g). ^{1}H NMR ^{1}H NMR ($CDCl_3$): δ = 1.45 (s, 36H), 2.8 (s, 3H), 2.6–2.9 (m, 3H), 3.1 (dd, ^3J = 14.7, 7.3 Hz, 1H), 3.30–3.50 (m, 6H), 3.6–3.85 ppm (m, 8H).

Preparation of H_5L1: A round-bottomed flask, equipped with an addition funnel and temperature probe was charged with phosphorous trichloride (102 µl) and THF (2 mL). A solution consisting of compound **4** (295 mg) in THF (3 mL) was added over a period of 35 min, while maintaining an internal temperature of −5 to 0 °C, and the mixture was then stirred for a further 30 min. A solution consisting of imidazole (400 mg) in THF (3 mL) was added over a period of 15 min, while maintaining an internal temperature of 0 to 5 °C and the mixture was stirred for 20 min. A solution consisting of compound **3** (706 mg) in a mixture of hexanes (1.5 mL) and THF (4.0 mL) was added over a period of 15 min, while maintaining an internal temperature of −5 to 0 °C. The mixture was stirred for 20 min. Water (3 mL) was added over a period of 5 min, while maintain-

ing an internal temperature 0–5 °C, and the mixture was stirred for 5 minutes. Hexanes (9 mL), toluene (1 mL), and aqueous HCl (5 N, 3 mL) were added over 5 min, while maintaining an internal temperature of 5–10 °C. Sodium periodate (175 mg) was added over a period of 3 min, while maintaining an internal temperature of 5–10 °C. The reaction mixture was warmed to room temperature over 15 min and stirred for an additional 30 min. The layers were separated and the organic layer was washed with 10 % aqueous sodium thiosulfate (2×5 mL mL). To the organic layer was added tetraoctylammonium bromide (63 mg). Concentrated HCl (6 mL) was then added over a period of 10 min, while maintaining an internal temperature of 20–25 °C. This mixture was stirred for 16 h. The layers were separated and the organic layer was discarded. Aqueous sodium hydroxide (8 M, 10 mL) was added to the aqueous layer until a pH of 6.5 was reached. The solution was concentrated under reduced pressure and then loaded onto a C-18 reverse-phase silica-gel-packed column for purification. Lyophilization provided compound L1 as a white powder (0.385 g). Elemental analysis calcd (%) for $C_{32}H_{44}N_3O_{12}P{\cdot}H_2O$: C 54.00, H 6.51, N 5.90, P 4.35, H_2O 2.53; found: C 53.88, H 6.75, N 5.91, P 4.56, H_2O 2.59; ES^+-MS: *m/z*: 694.3 [M^++H]. ^{1}H NMR (D_2O/NaOD): δ = 2.88 (H-1), 3.69 (H-2a), 3.83 (H-2b), 2.56 (H-3a), 2.23 (H-3b), 2.63 (H-4a), 2.52 (H-4b), 2.19 (H-5), 3.26 (H-6a), 2.95 (H-6b), 2.50 (H-7a), 2.21 (H-7b), 4.17 (H-8), 2.56 (H-9a), 2.11 (H-9b), 1.82 (H-10a), 1.58 (H-10b), 7.25 (H-14), 7.33 (H-15), 7.14 ppm (H-16); ^{13}C NMR (D_2O/NaOD): δ = 60.7 (C-1), 62.9 (C-2), 54.5(C-3), 51.7 (C-4), 38.1 (C-5),58.3 (C-6), 51.7 (C-7),74.3 (C-8),32.5 (C-9/9′), 29.5 (C-10/10′), 58.4 (C-11), 58.3 (C-12/13), 128.6 (C-14), 126.1 (C-15),126.8 ppm (C-16).

Preparation of Gd–L1: The concentration of the ligand **L1** was determined by photometric titration with $Gd(NO_3)_3$ as described previously.[6] A solution of $GdCl_3$ (0.447 mL, 150.9 mM, 67.5 μmol) was added to a solution of **L1** (1.09 mL, 61.5 mM, 67.3 μmol) at pH 6.8, and the pH adjusted to 6.8 using 1 M NaOH. The solution was stirred for 30 min and then lyophilized affording crude chelate. Inorganic impurities were removed by elution through a pre-packed and equilibrated C18 column with a gradient of water to 1:1 ethanol/water and conductivity detection. Ethanol was removed by rotary evaporation and the remaining aqueous solution was lyophilized to afford purified chelate **Gd–L1** as the pentahydrate disodium salt as a white solid (46.7 mg, 71 %). Elemental analysis calcd (%) for $C_{32}H_{39}GdNa_2N_3O_{12}P{\cdot}5H_2O$: C 39.14, H 5.03, N 4.28, Na 4.68, P 3.15; found: C 39.40, H 5.19, N 4.33, Na 4.93, P 3.18. An aqueous solution of **Gd–L1** on a HPLC-MS with UV (254 nm) and +ESI detection with a gradient of 50 mM ammonium formate with 2 % (9:1 MeCN/50 mM ammonium formate) rising to 50 % (9:1 MeCN/50 mM ammonium formate) over 5 min (0.8 mL min^{-1}, Kromasil C4, 50×4.6 mm, 3.5 μm) elutes at 3.39 min (97.3 % total peak area at 254 nm, positive ion, *m/z* = 849.2 [M^+ +2H]). There was no detectable **L1** (**L1** elutes at 3.16 min. under the same conditions) or unchelated gadolinium (xylenol orange test).

Determination of protonation and metal–ligand stability constants: Titration pH measurements of H_5**L1** in the absence and presence of Gd^{III}, Ca^{II}, and Zn^{II} were performed with a Fisher Accumet 25 pH meter equipped with an Orion Ross combination semimicro electrode. The electrode was calibrated before each titration by titrating a known amount of standardized $HClO_4$(aq) with standardized NaOH solution at an ionic strength of 0.1 M using $NaClO_4$ as the inert electrolyte. A plot of mV (measured) versus pH (calculated) gave a working slope and intercept so that pH could be read as −log[H^+] directly. In this report, pH refers to the hydrogen ion concentration and not activity. A Metrohm automatic buret (Dosimat 665) was used for the NaOH additions and the buret and pH meter were interfaced to a PC such that each titration was automated by using the program TITRATE.[17] The temperature of each solution, maintained in a covered, water-jacketed vessel, was kept constant at 25.0±0.1 °C by a Fisher Isotemp 901 circulating bath. The ionic strength was kept constant at 0.10 M $NaClO_4$. Nitrogen, after passage through 30 % NaOH, was bubbled through the solutions to exclude carbon dioxide.

Distilled deionized water (Nanopure, Barnstead) was used for all solutions. Solutions of the ligand were prepared by dissolving a weighed quantity into a known volume of 0.1 M $NaClO_4$. The concentration was calculated based on the molecular weight of the complex and was confirmed by titration. There are two inflections in the ligand titration curve and two equivalents of hydroxide were required to span these two inflections. Perchlorate stock solutions of Gd^{III}, Ca^{II}, and Zn^{II} were prepared by dissolving a known amount of the oxide in a slight excess of perchloric acid and diluting to a known volume. Because hydrolysis of these metal ions occurs at pH >5, the excess acid concentration was determined directly by titration with standard NaOH and analysis by Gran's method.[18] Sodium hydroxide solutions (0.1 M) were prepared from dilution of 50 % NaOH with freshly boiled distilled, deionized water that had been saturated with argon. The base solutions were standardized against potassium hydrogen phthalate. The amount of carbonate present in the NaOH solutions was estimated from Gran plots[18] and was always less than 1 %. Acid solutions were standardized against standard NaOH.

The ligand solutions (1–2 mM) were titrated with NaOH over a pH range from 2–11 collecting about 110 data points per titration. The titration data was fit to a model of a ligand with five ionizable groups by using the program BEST.[19] The value of pK_w was fixed at 13.78 for all analyses.[20] Equimolar metal–ligand solutions were titrated (110 data points per titration) over the pH range 2–11 with NaOH for Ca^{II} and Zn^{II}, and the stability constants determined by analysis of the titration curve with BEST.[19] The Ca^{II} data was fit to a model containing two metal–ligand species: **Ca–L1**, and **HCa–L1**. The Zn^{II} data was modeled with three metal–ligand species: **Zn–L1**, **HZn–L1**, and **H_2Zn–L1**. Multinuclear species were not included in the models; since the metal/ligand stoichiometry was 1:1 and the data was well reproduced using the species described. For Gd^{III}, aqueous solutions containing 1:1 or 2:1 mixtures of **L1** and Gd^{III} formed precipitates at pH lower than 2.7. Above pH 2.7 only one species was observed, **Gd–L1**. The precipitation at low pH made it impossible to work under conditions in which there was a significant fraction of unchelated Gd^{III}. To circumvent this problem, a competition study was carried out by using an EDTA competitor ligand and monitoring the equilibrium by HPLC-MS with a reverse-phase column and eluting with a pH 6.8 NH_4OAc buffer. Six solutions were prepared containing 1 part **L1** to 1 part Gd^{III} to 0.75–1.25 parts EDTA with pH ranging from 3.1 to 3.4. The pH reading stabilized within minutes; however, care was taken to ensure that there was no slow pH drift due to slow transmetallation kinetics. Under these conditions, [Gd(EDTA)] and EDTA eluted in the void volume while **L1** (3.42 min) and **Gd–L1** (2.80 min) were retained (EDTA = ethylenediaminetetraacetate). This allowed the determination of the distribution of Gd^{III} in the system, and the formation constant for **Gd–L1** was determined by solving the appropriate mass balance equations using the protonation constants for **L1** and EDTA and the [Gd(EDTA)] stability constant.[20]

ENDOR spectroscopy: The pulsed EPR experiments were performed with frozen (8 K) solutions of 1 mM **Gd–L1** in 1:1 (v/v) H_2O/CD_3OH (methanol added for glassification). In these experiments, which included the electron spin echo (ESE) field sweep and Mims ENDOR[21] measurements, the D-band (130 GHz) spectrometer[22] of Argonne National Laboratory was used. ^{1}H ENDOR spectra were acquired at the maximum of the EPR spectrum (at which all EPR transitions contribute, but the −1/2↔+1/2 transition dominates) and at 24 mT lower B_0 (at which all EPR transitions contribute except the −1/2↔+1/2 transition). Subtracting the latter spectrum from the former gives, after appropriate normalization, the spectrum associated with solely the −1/2↔+1/2 electron-spin transition. The data were analyzed as described previously[23–25] to extract $Gd{-}H_{water}$ distance estimates.

Ultrafiltration measurements of binding: Solutions containing 0.1 mM Gd^{III} chelate and human serum albumin (4.5 % w/v) were prepared by mixing appropriate volumes of **Gd–L1** or **Gd–L2** stock solution, 6 % HSA and PBS. Two aliquots (400 μL) of each these samples were placed in 5 kDa ultrafiltration units. Two additional 25 μL aliquots were analyzed by ICP-MS to determine the total Gd concentration. The samples were incubated at 37 °C for 10 min, and then centrifuged at 5800 g for 3.5 min. The filtrates (~30 μL) from these ultrafiltration units were used to determine the free concentration of complex in each of the samples by ICP-MS.

Relaxivity: Relaxivities were determined at 20 MHz (0.47 T) by using a Bruker Minispec NMS 120 to determine T_1. T_1 was measured with an in-

version recovery pulse sequence and all samples were measured at 37 °C. Relaxivity was obtained from the slope of a plot of $1/T_1$ versus concentration for 0, 20, 40, and 60 μM Gd samples in 660 μM HSA. Relaxivities in HEPES (pH 7.4) buffer were determined using solutions of 0, 100, 150, and 200 μM Gd (HEPES = 2-[4-(2-hydroxyethyl)-1-piperazinyl]ethanesulfonic acid). The ^{1}H NMRD profiles (5, 35 °C) were recorded on a field cycling relaxometer at NY Medical College over the frequency range 0.01 to 50 MHz. For the samples in HSA, the gadolinium concentration was 100 μM and the HSA was 660 μM. For the HEPES buffer only solutions, the Gd^{III} concentration was 1 mM. Relaxivity was computed by subtracting the relaxation rate of the medium (HSA in HEPES, or HEPES only) from the relaxation rate of the Gd solution at each field strength and dividing the difference by the gadolinium in millimoles. All solutions were assayed for gadolinium concentration by ICP-MS.

^{17}O NMR: $H_2{}^{17}O$ transverse relaxation rates were determined for a HEPES buffer solution in the presence and absence of 9.399 mmolal **Gd–L1** as a function of temperature (−7 to 95 °C) on a Varian Unity 300 NMR operating at 40.6 MHz. Probe temperatures were determined from ethylene glycol or methanol chemical shift calibration curves. T_2 was determined by a CPMG pulse sequence. Measurements were repeated after heating to ensure reproducibility. The variable-temperature relaxation-rate data was analyzed as described previously[6] to extract water exchange and rotational dynamics parameters.

Acknowledgements

We would like to acknowledge the many contributions to the field of MRI contrast agent research and to chemistry as a whole by Professor André Merbach. One of us (P.C.) is extremely appreciative of having had Professor Merbach as a mentor. The work done at Argonne National Laboratory was supported by the U.S. Department of Energy, Office of Basic Energy Sciences, Division of Chemical Sciences, under Contract W-31-109-Eng-38.

[1] R. R. Edelman, J. R. Hesselink, M. B. Zlatkin, *MRI: Clinical Magnetic Resonance Imaging*, Saunders, Philadelphia, **1996**.
[2] P. Caravan, J. J. Ellison, T. J. McMurry, R. B. Lauffer, *Chem. Rev.* **1999**, *99*, 2293–2352.
[3] H. Gries, *Top. Curr. Chem.* **2002**, *221*, 1–24.
[4] R. B. Lauffer, D. J. Parmelee, S. U. Dunham, H. S. Ouellet, R. P. Dolan, S. Witte, T. J. McMurry, R. C. Walovitch, *Radiology* **1998**, *207*, 529–538.
[5] D. A. Bluemke, A. E. Stillman, K. G. Bis, T. M. Grist, R. A. Baum, R. D'Agostino, E. S. Malden, J. A. Pierro, E. K. Yucel, *Radiology* **2001**, *219*, 114–122.
[6] P. Caravan, N. J. Cloutier, M. T. Greenfield, S. A. McDermid, S. U. Dunham, J. W. Bulte, J. C. Amedio, Jr., R. J. Looby, R. M. Supkowski, W. D. Horrocks, Jr., T. J. McMurry, R. B. Lauffer, *J. Am. Chem. Soc.* **2002**, *124*, 3152–3162.
[7] T. J. Swift, R. E. Connick, *J. Chem. Phys.* **1962**, *37*, 307–320.
[8] R. B. Lauffer, *Chem. Rev.* **1987**, *87*, 901–927.
[9] K. Micskei, L. Helm, E. Brucher, A. E. Merbach, *Inorg. Chem.* **1993**, *32*, 3844–3850.
[10] K. Micskei, D. H. Powell, L. Helm, E. Brucher, A. E. Merbach, *Magn. Reson. Chem.* **1993**, *31*, 1011–1020.
[11] G. Gonzalez, D. H. Powell, V. Tissieres, A. E. Merbach, *J. Phys. Chem.* **1994**, *98*, 53–59.
[12] D. H. Powell, O. M. Ni Dhubhghaill, D. Pubanz, L. Helm, Y. S. Lebedev, W. Schlaepfer, A. E. Merbach, *J. Am. Chem. Soc.* **1996**, *118*, 9333–9346.
[13] E. Toth, D. Pubanz, S. Vauthey, L. Helm, A. E. Merbach, *Chem. Eur. J.* **1996**, *2*, 1607–1615.
[14] E. Toth, F. Connac, L. Helm, K. Adzamli, A. E. Merbach, *Eur. J. Inorg. Chem.* **1998**, 2017–2021.
[15] T. J. McMurry, D. J. Parmelee, H. Sajiki, D. M. Scott, H. S. Ouellet, R. C. Walovitch, Z. Tyeklar, S. Dumas, P. Bernard, S. Nadler, K. Midelfort, M. Greenfield, J. Troughton, R. B. Lauffer, *J. Med. Chem.* **2002**, *45*, 3465–3474.
[16] J. C. Amedio, Jr., P. J. Bernard, M. Fountain, G. Van Wagenen, Jr., *Synth. Commun.* **1999**, *29*, 2377–2391.
[17] S. M. Rocklage, S. H. Sheffer, W. P. Cacheris, S. C. Quay, E. F. Hahn, K. N. Raymond, *Inorg. Chem.* **1988**, *27*, 3530–3534.
[18] G. Gran, *Acta Chem. Scand.* **1950**, *4*, 559–577.
[19] R. J. Motekaitis, A. E. Martell, *Can. J. Chem.* **1982**, *60*, 2403.
[20] A. E. Martell, R. M. Smith, R. J. Motekaitis, *NIST Critically Selected Stability Constants of Metal Complexes: NIST Standard Reference Data 46*, National Institute of Standards and Technology, Washington, DC, **1997**.
[21] W. B. Mims, *Proc. R. Soc. London Ser. A* **1965**, *283*, 452.
[22] K. V. Lakshmi, M. J. Reifler, G. W. Brudvig, O. G. Poluektov, A. M. Wagner, M. C. Thurnauer, *J. Phys. Chem. B* **2000**, *104*, 10445–10448.
[23] A. V. Astashkin, A. M. Raitsimring, P. Caravan, *J. Phys. Chem. A* **2004**, *108*, 1900–2001.
[24] A. M. Raitsimring, A. V. Astashkin, D. Baute, D. Goldfarb, P. Caravan, *J. Phys. Chem. A* **2004**, *108*, 7318–7323.
[25] P. Caravan, A. V. Astashkin, A. M. Raitsimring, *Inorg. Chem.* **2003**, *42*, 3972–3974.
[26] P. Caravan, C. Comuzzi, W. Crooks, T. J. McMurry, G. R. Choppin, S. R. Woulfe, *Inorg. Chem.* **2001**, *40*, 2170–2176.
[27] W. P. Cacheris, S. C. Quay, S. M. Rocklage, *Magn. Reson. Imaging* **1990**, *8*, 467–481.
[28] P. L. Anelli, V. Balzani, L. Prodi, F. Uggeri, *Gazz. Chim. Ital.* **1991**, *121*, 359–364.
[29] M. C. Alpoim, A. M. Urbano, C. F. G. C. Geraldes, J. A. Peters, *J. Chem. Soc. Dalton Trans.* **1992**, 463–467.
[30] C. C. Bryden, C. N. Reilley, *Anal. Chem.* **1982**, *54*, 610–615.
[31] C. A. Chang, H. G. Brittain, J. Telser, M. F. Tweedle, *Inorg. Chem.* **1990**, *29*, 4468–4473.
[32] C. F. G. C. Geraldes, A. D. Sherry, W. P. Cacheris, K. T. Kuan, R. D. Brown, III, S. H. Koenig, M. Spiller, *Magn. Reson. Med.* **1988**, *8*, 191–199.
[33] S. Aime, M. Botta, S. G. Crich, G. Giovenzana, R. Pagliarin, M. Sisti, E. Terreno, *Magn. Reson. Chem.* **1998**, *36*, S200-S208.

Received: March 25, 2005
Published online: July 29, 2005

